Sensors and Materials, Vol. 35, No. 11 (2023) 3807–3828
MYU Tokyo

S & M 3452

Uncertainty Analysis of Particle Backscattering Coefficient Measurement for Multiple Highly Turbid Water Areas in Ocean Color Remote Sensing

Hiroto Higa,[1*] Ryota Ideno,[1] Salem Ibrahim Salem,[2,3] and Hiroshi Kobayashi[4]

[1]Institute of Urban Innovation, Yokohama National University,
Hodogaya, Yokohama, Kanagawa 240-8501, Japan
[2]Faculty of Engineering, Kyoto University of Advanced Science,
18 Yamanouchi Gotanda-cho, Ukyo-ku, Kyoto 615-8577, Japan
[3]Faculty of Engineering, Alexandria University,
Lotfy El-Sied St. off Gamal Abd El-Naser-Alexandria, Alexandria Governorate 11432, Egypt
[4]Division of Life and Environmental Sciences, University of Yamanashi,
Takeda, Kofu, Yamanashi 400-8510, Japan

(Received July 11, 2023; accepted October 19, 2023)

Keywords: backscattering coefficient, Hydroscat-6P, σ correction, Hydrolight

In this study, we aimed to understand the uncertainty of measured values of the particle backscattering coefficient (b_{bp}) obtained using the *in situ* backscattering meter Hydroscat-6P in three highly turbid water bodies with distinct optical properties and assess their impact on the estimation results through inversion. The field observations were conducted in Tokyo Bay, where organic matter dominates, Lake Kasumigaura, where cyanobacteria are abundant and mixed with inorganic suspended matter, and the estuary of Bangpankong River in the Upper Gulf of Thailand, where inorganic suspended matter is highly concentrated. To understand the uncertainty of b_{bp} measurements, radiative transfer simulations were performed using Hydrolight, and the influence of b_{bp} measurements on the reproduction calculation of remote sensing reflectance (R_{rs}) was assessed. The results revealed that the reproducibility of R_{rs} varied among the water bodies, with a particularly pronounced overestimation compared with the measured values in the highly scattering environments of Lake Kasumigaura and the Upper Gulf of Thailand. This overestimation originated from the optical path length without light attenuation correction (σ correction) in Hydroscat-6P, and the σ correction amplified the overestimation of R_{rs}. Although the cause of this overestimation is unclear, it suggests that the calculation conditions of the radiative transfer model and the effect of multiple scattering between the sensors of Hydroscat-6P may be contributing factors. The magnitude of this overestimation ranged from 64 to 75% in Lake Kasumigaura and from 29 to 39% in the Upper Gulf of Thailand, significantly affecting the accuracy verification of b_{bp} estimation using inversion models. These results highlight the uncertainty of b_{bp} measurements in highly turbid water bodies with high light scattering, emphasizing the need for careful attention to the quality of previously acquired *in situ* data when evaluating the performance of inversion algorithms.

*Corresponding author: e-mail: higa@ynu.ac.jp
https://doi.org/10.18494/SAM4576

ISSN 0914-4935
https://myukk.org/

1. Introduction

In ocean color remote sensing, the inherent optical properties (IOPs) represent the absorption and scattering of light dependent on water and its constituents. IOPs are important parameters for understanding the physical, biological, and chemical properties of marine substances, and numerous estimation algorithms have been proposed in previous studies.[1] One of the IOPs, the backscattering coefficient (b_{bp}), is a parameter obtained by integrating the volume scattering function (VSF) over the backward hemisphere and varies with the size, shape, and composition of the substances in the water. Particularly in coastal areas, it has been reported that scattering characteristics vary owing to the occurrence of highly scattering phytoplankton and the concentrations, particle sizes, and compositions of inorganic suspended solids such as sand. In highly turbid water areas with various substances mixed together, these variations are considered to become more complex.[2]

In such highly turbid water areas, the decrease in estimation accuracy by inversion models of IOPs has been a concern.[3,4] At the same time, uncertainties in the measurement of b_{bp} itself have been pointed out.[5] Various methods have been proposed for measuring b_{bp}, and among them, commercially available field-type backscattering meters have been widely used in many studies and employed for radiative transfer calculations and validation of IOP estimation models.[6,7] One of these field-type backscattering meters is the Hydroscat series by HOBI Labs, Inc., which enables simple measurement of b_{bp} in the field and has been utilized in many studies. [8,9] In the measurement of b_{bp} using the Hydroscat series, the sensor of the instrument measures the VSF at a fixed angle of 140° [β (140)] in multiple spectral bands. The conversion coefficient χ is then used to convert the VSF at a fixed angle to b_{bp}.[10,11]

In general, field-type backscattering measurement devices such as Hydroscat require correction methods to account for the attenuation of light along the optical path between the emission of light from the light emitting diode and its reception at the photodiode. In the case of Hydroscat, a correction method called σ correction has been proposed, which evaluates and adds the attenuation component of scattered light along the optical path.[11] However, it has been pointed out that errors in b_{bp} measurement occur during the σ correction stage in highly turbid water areas,[12] and new correction methods suitable for such areas have also been proposed.[5] For these correction methods, including the σ correction, it is important to determine the optical characteristics of the water area in advance and apply the appropriate method. However, the applicability of these methods to water areas with different optical characteristics has not been clearly established. Furthermore, in previous studies, to verify the measurement accuracy of b_{bp}, radiative transfer models have been used to calculate apparent optical properties such as remote sensing reflectance (R_{rs}) using IOPs as input values, and these calculated values are compared with the measured values.[5,13,14] The calculation conditions for the absorption coefficients and the angular distribution of scattering in radiative transfer calculations ideally should use measured values. However, there are often limited examples where all parameters are measured, and it is important to evaluate the effect of differences in calculation conditions on the calculation accuracy using the limited measured values. Furthermore, the uncertainty of the measured values of b_{bp} may also lead to incorrect interpretations of the validation results of inversion models, highlighting the importance of understanding its impact.

Therefore, in this study, we aim to assess the uncertainties in b_{bp} measurements using the field-type backscattering instrument Hydroscat-6P in three highly turbid water areas with significantly different optical characteristics: Tokyo Bay, Lake Kasumigaura, and the mouth of Bangpankong River in the Upper Gulf of Thailand. The characteristics of b_{bp} measurements and the tendencies for uncertainty in each water area were investigated by comparing the calculated values of R_{rs} using the radiative transfer model Hydrolight with the measured values. Furthermore, the impact of uncertainties in b_{bp} measurements on the validation results of the inversion models in each water area was assessed. In this study, the definition of high-turbidity water areas refers to regions where organic and inorganic suspended matter coexist, leading to a high concentration of particulate matter in the water.

2. Materials and Methods

2.1 Field observations

In this study, optical and water quality observations were conducted at the observation sites shown in Fig. 1, focusing on Tokyo Bay and Lake Kasumigaura in Japan, and the estuary of the Bangpankong River in the Upper Gulf of Thailand (referred to as the Upper Gulf of Thailand). In Tokyo Bay, a total of 10 observation campaigns (N = 49) were conducted between September

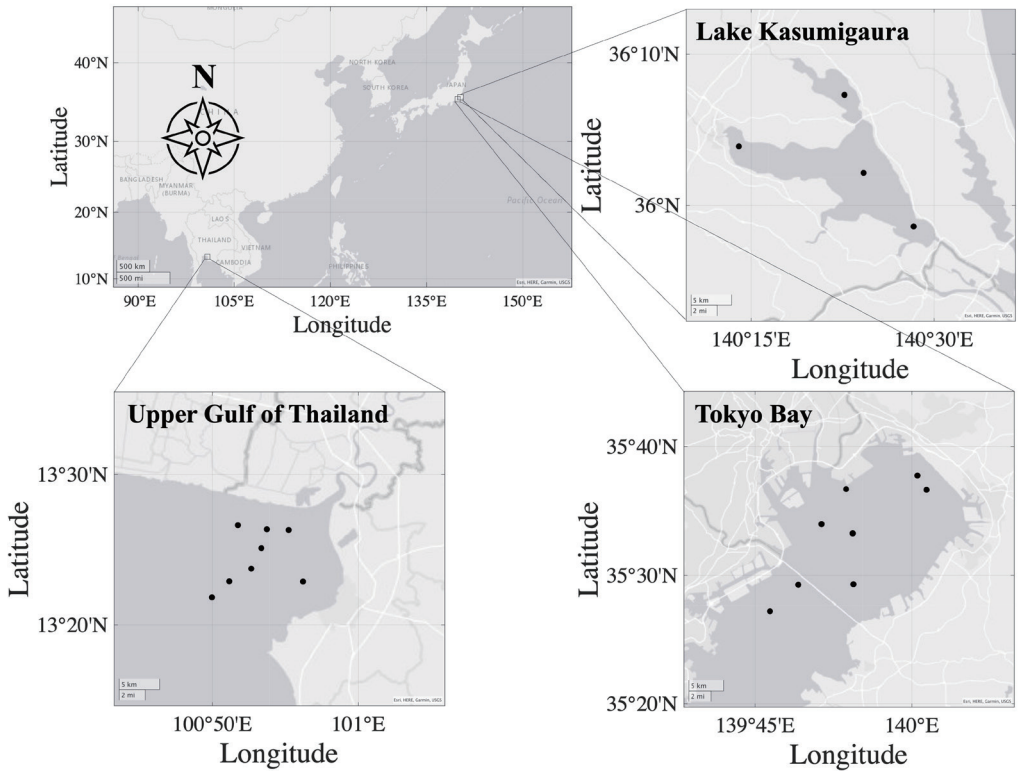

Fig. 1. Observation sites in Tokyo Bay, Lake Kasumigaura and at the estuary of Bangpankong River, Upper Gulf of Thailand

2011 and September 2022. In Lake Kasumigaura, three observation campaigns (N = 12) took place between August 2017 and August 2018. In the Upper Gulf of Thailand, one observation campaign (N = 8) was conducted in July 2011.

Tokyo Bay is located between approximately 35.45 to 35.62°N latitude and 139.77 to 140.02°E longitude, with a north–south extent of 50 km and an east–west extent of 10–30 km, covering an area of 960 km². The bay is highly eutrophic with significant organic pollution, and red tides occur approximately 70 times per year. Lake Kasumigaura is the second largest lake in Japan, located between approximately 35.97 to 36.12°N latitude and 139.77 to 140.02°E longitude. It has a surface area of 168 km², a water volume of 800×10^6 m³, and a catchment area of 220 km². The lake is shallow with an average depth of 4.0 m. The water level of the lake is controlled by gates at its outlet, and it takes about 200 days to replace the lake water. The lake is also eutrophic, and occurrences of *Microcystis*-dominated cyanobacterial blooms have been reported. The estuary of Bangpankong River in the Upper Gulf of Thailand is located between approximately 13.30 to 13.15°N latitude and 100.45 to 101.00°E longitude. In the river mouth area, inorganic suspended matter dominates, resulting in significant light scattering.[15]

In the measurement of b_{bp}, the Hydroscat-6P instrument from HOBI Labs, Inc. was deployed vertically from a ship to measure the vertical profiles of β (140) at six wavelengths: 420, 442, 488, 510, 550, and 676 nm. The measured β (140) values were converted to b_{bp} by the method described in Sect. 2.2. In this study, the vertical profiles of b_{bp} were examined, and any sudden abnormal values were removed. The average values from depths of 0.5 to 1.5 m were used as the surface b_{bp} values.

For the measurement of absorption coefficients, water samples were collected at each location. Subsequently, 25 mm Whatman Grade GF/F filters with a pore size of 0.7 μm were used to measure the phytoplankton absorption (a_{ph}) and the non-algal particle absorption (a_{NAP}) using a spectrophotometer (JASCO V-550) based on the filter pad method. The colored dissolved organic matter absorption (a_{CDOM}) was measured by filtering through 47 mm Whatman Grade GF/F filters with a pore size of 0.7 μm, followed by sequential filtration through 47 mm Nuclepore membrane filters with a pore size of 0.4 μm and 47 mm Nuclepore membrane filters with a pore size of 0.2 μm. The filtrate was then transferred to a 14 cm quartz cell with a diameter of 25 mm for measurement using the spectrophotometer (JASCO V-550).

For the measurement of apparent optical properties, such as upwelling radiance and downwelling irradiance, the TriOS RAMSES ARC/ACC instrument was used, and the ratio R_{rs} was calculated. The chlorophyll-a (Chl-a) concentration was measured using a fluorometer (Turner Designs 10-AU-005-CE). Total suspended solids (TSS) and inorganic suspended solids (ISS) were measured by the dry weight method.

2.2 Calculation method of backscattering coefficient

The field-deployable backscattering instrument used in this study, Hydroscat-6P, measures b_{bp} at six wavelengths using a 140° scattering light measurement method. The instrument consists of an emitter and a receiver located at the bottom. The emitter emits light from an LED, forming a sampling volume in the water, while the receiver's photodiode measures the volume

scattering function β (140) by detecting the scattered light at 140°. Along the optical path between the emitter and receiver, the emitted light is attenuated by water and substances present in the water, resulting in light attenuation. The σ correction method is used to account for the attenuation caused by light scattering. In the σ correction, the following equation considers the effect of light attenuation:

$$\beta(140) = k_1 \exp\left(k_{exp} \times k_{bb}\right) \times \beta_u(140). \tag{1}$$

k_1 is set to 1 for practical purposes at all wavelengths. k_{exp} represents the wavelength-dependent optical path length between the emitter and receiver, β_u is the measured volume scattering function, and β is the volume scattering function after σ correction is applied. Here, σ (k_{bb}) is expressed as σ (k_{bb}) = $k_1$exp (k_{exp} × k_{bb}), where σ (k_{bb}) represents the σ coefficient. k_{bb} is the attenuation coefficient of light along the optical path, and it is described by the following equation as reported by HOBI Labs, Inc. (2008).[16]

$$k_{bb} = a_{nw} + 0.4 \times b_p \tag{2}$$

Here, a_{nw} represents the nonwater-contributed absorption coefficient, and b_p represents the nonwater-contributed scattering coefficient. b_p can be calculated using the following equation:

$$b_p = (b_{bu} - b_{bw}) / B. \tag{3}$$

Here, b_{bu} is the backscattering coefficient before correction, b_{bw} is the backscattering coefficient of water, and B is the backscattering probability. In previous studies, the actual measured values of b_p were used, and methods for calculating k_{bb} were employed.[17] However, instruments such as the absorption and attenuation meter (AC-9) and AC-spectral absorption and attenuation sensor (AC-S), which are used to measure b_p, have uncertainties in the correction for light attenuation in highly turbid waters.[12] Additionally, in commonly available optical datasets, data for b_p are often not measured. Therefore, in this study, reference was made to HOBI Labs, Inc. (2008),[16] and B was set to a constant value of 0.015. The a_{nw} in Eq. (2) was determined using measured values. The conversion from β to b_{bp} was performed using a scaling factor χ, as shown in the following equation. When no σ correction is applied, it is denoted as $b_{bp,u}$ and expressed as shown in Eq. (5).

$$b_{bp} = 2\pi \times \chi \times \left(\beta(140) - \beta_w(140)\right) \tag{4}$$

$$b_{bp,u} = 2\pi \times \chi \times \left(\beta_u(140) - \beta_w(140)\right) \tag{5}$$

b_b is obtained by integrating the volume scattering function over the backward hemisphere. Using the mean value theorem of integration, it can be expressed as $b_b = 2\pi\beta(\theta)$ using the volume scattering function $\beta(\theta)$ at a certain angle θ. A scaling factor χ has been proposed to calculate b_b from the volume scattering function at a specific angle.[10] In this study, χ = 1.08 was used for β (140).[16]

2.3 Radiative transfer model and IOP inversion model

In this study, we conducted an accuracy assessment of the measured values of b_p using the radiative transfer model Hydrolight 6.0.[18] The radiative transfer model solves the one-dimensional and time-independent radiative transfer equation in the vertical direction of the water column to calculate the distribution of radiance in a parallel plane in the marine area. The input value for the beam attenuation coefficient (c) was calculated as the sum of the measured total absorption coefficient (a) and the total scattering coefficient (b). The total scattering coefficient was converted by adding the contribution of backscattering by water to Eq. (4) and then dividing it by a value equivalent to the parameter B used in Eq. (3). It was then calculated as the sum of a measured value. The phase function was represented using the Fournier–Forand phase function[19] to express the scattering characteristics with respect to B. The solar zenith angle and wind speed were set to constant values of 30° and 5.0 m/s, respectively. Furthermore, for the boundary conditions at the seafloor, considering the high turbidity and large water depths in the three study areas, it was assumed that light does not reach the seafloor and the calculations were performed with an infinite water depth. The calculation wavelengths were set to the six wavelengths measured by Hydroscat-6P, and chlorophyll fluorescence was taken into account using the model proposed by Gilerson *et al.*[20]

The IOP inversion model, based on the Bio-Optical model, used the Quasi-Analytical Algorithm v6[21] to estimate the IOPs step by step. This allowed us to assess the influence of the uncertainty in the measured values on the accuracy of b_{bp} estimation.

2.4 Error metrics

The comparison between the estimated b_{bp} obtained through QAA, the calculated R_{rs} using the radiative transfer model, and their respective measured values was evaluated using two error metrics: root mean square logarithmic error (*RMSLE*) and *Bias*.

$$RMSLE = \left[\frac{1}{N} \sum_{i=1}^{N} \left(\log_{10}\left(X_i^E\right) - \log_{10}\left(X_i^M\right) \right)^2 \right]^{\frac{1}{2}} \tag{6}$$

$$Bias = \frac{1}{N} \sum\nolimits_{i=1}^{N} (X_i^E - X_i^M) \tag{7}$$

Here, N represents the number of samples, X_i^E denotes the estimated values obtained from the model, and X_i^M represents the corresponding measured values.

3. Results

3.1 Field observation results

Table 1 presents the statistical indicators of water quality and IOPs for each study area, Fig. 2 shows the spectral distribution of R_{rs} for each study area, and Fig. 3 depicts the spectral distribution of b_{bp}. When comparing the spectral distributions of R_{rs} for each study area, the intensity of R_{rs} at 550 nm is approximately three times greater in Lake Kasumigaura and the Upper Gulf of Thailand than in Tokyo Bay. On the other hand, the average value of b_{bp} at 550 nm in Lake Kasumigaura and the Upper Gulf of Thailand is more than ten times higher than that in Tokyo Bay, suggesting an increase in R_{rs} owing to the effect of light scattering. Although the difference in the average values of Chl-a between Tokyo Bay and Lake Kasumigaura is small, it is evident that the maximum Chl-a in Tokyo Bay reaches a high level of 93.6 mg/l. In a

Table 1
Minimum, maximum, mean, and standard deviation (SD) values of water quality parameters (Chl-a, TSS, OSS, ISS) and IOPs [a_{ph} (443), a_{CDOM} (443), a_{NAP} (443), b_{bp} (443), b_{bp} (550)] for Tokyo Bay, Lake Kasumigaura, and the Upper Gulf of Thailand.

	Minimum	Maximum	Mean	SD
Tokyo Bay (N = 43)				
Chl-a (mg/m^3)	2.90	93.64	28.80	27.90
TSS (g/m^3)	2.99	23.43	10.79	5.51
OSS (g/m^3)	0.32	13.35	5.66	3.26
ISS (g/m^3)	0.81	12.54	5.14	2.80
a_{ph} (443) (/m)	0.23	4.00	1.15	0.83
a_{CDOM} (443) (/m)	0.06	0.67	0.31	0.14
a_{NAP} (443) (/m)	0.10	4.43	0.62	0.88
b_{bp} (443) (/m)	0.009	0.100	0.034	0.019
b_{bp} (550) (/m)	0.006	0.064	0.027	0.013
Lake Kasumigaura (N = 12)				
Chl-a (mg/m^3)	16.32	43.27	26.06	8.33
TSS (g/m^3)	17.61	33.75	25.54	5.95
OSS (g/m^3)	5.08	8.16	6.86	1.25
ISS (g/m^3)	11.82	26.00	18.68	5.34
a_{ph} (443) (m^{-1})	0.28	1.48	0.68	0.38
a_{CDOM} (443) (m^{-1})	0.09	1.48	0.81	0.54
a_{NAP} (443) (m^{-1})	0.48	1.03	0.76	0.19
b_{bp} (443) (m^{-1})	0.168	0.590	0.342	0.149
b_{bp} (550) (m^{-1})	0.177	0.530	0.328	0.133
Upper Gulf of Thailand (N = 8)				
Chl-a (mg/m^3)	3.05	32.00	13.46	11.91
TSS (g/m^3)	2.70	32.60	14.61	10.53
OSS (g/m^3)	0.80	4.40	2.51	1.33
ISS (g/m^3)	1.70	28.10	12.09	9.25
a_{ph} (443) (m^{-1})	0.21	1.41	0.64	0.43
a_{CDOM} (443) (m^{-1})	0.06	0.43	0.20	0.13
a_{NAP} (443) (m^{-1})	0.33	2.07	1.01	0.61
b_{bp} (443) (m^{-1})	0.045	0.881	0.356	0.265
b_{bp} (550) (m^{-1})	0.036	0.711	0.288	0.218

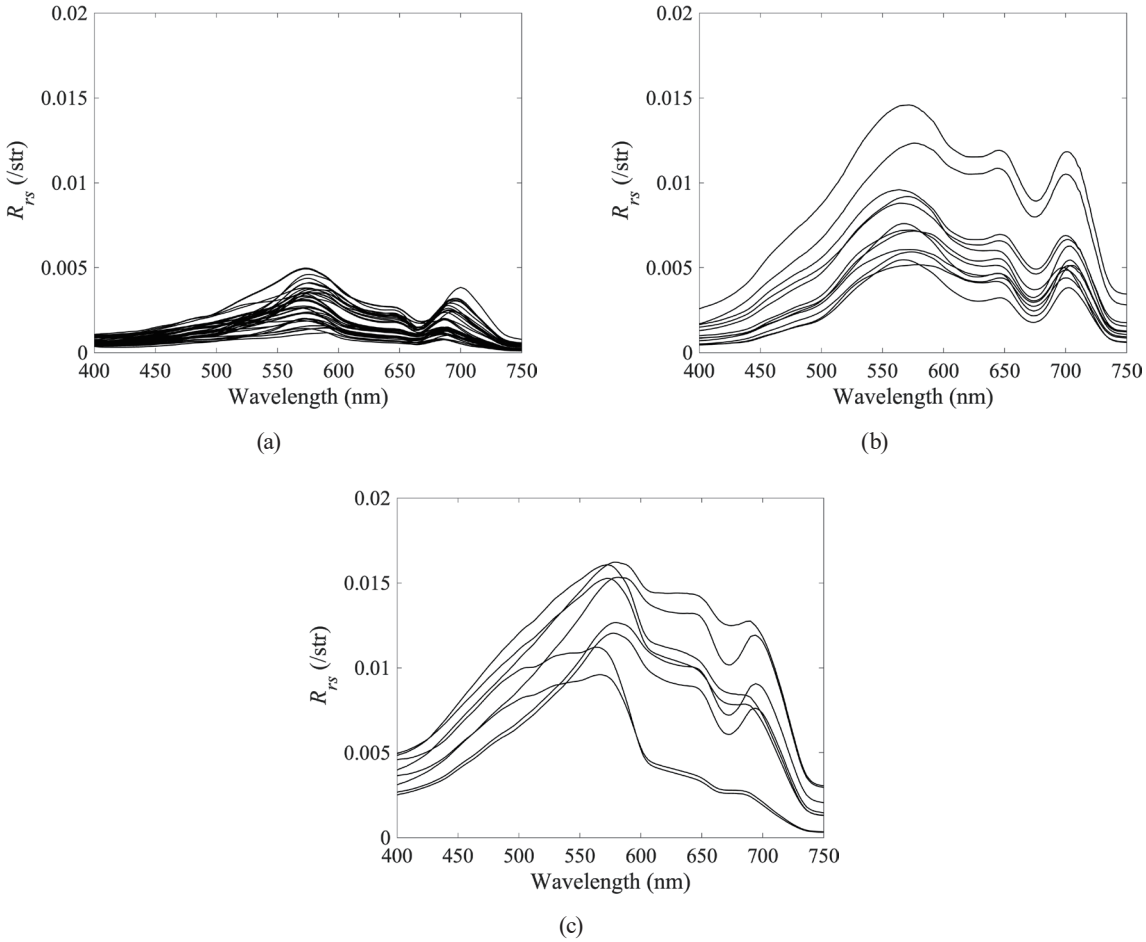

Fig. 2. Spectral distribution of R_{rs} in each water body. (a) Tokyo Bay, (b) Lake Kasumigaura, and (c) Upper Gulf of Thailand.

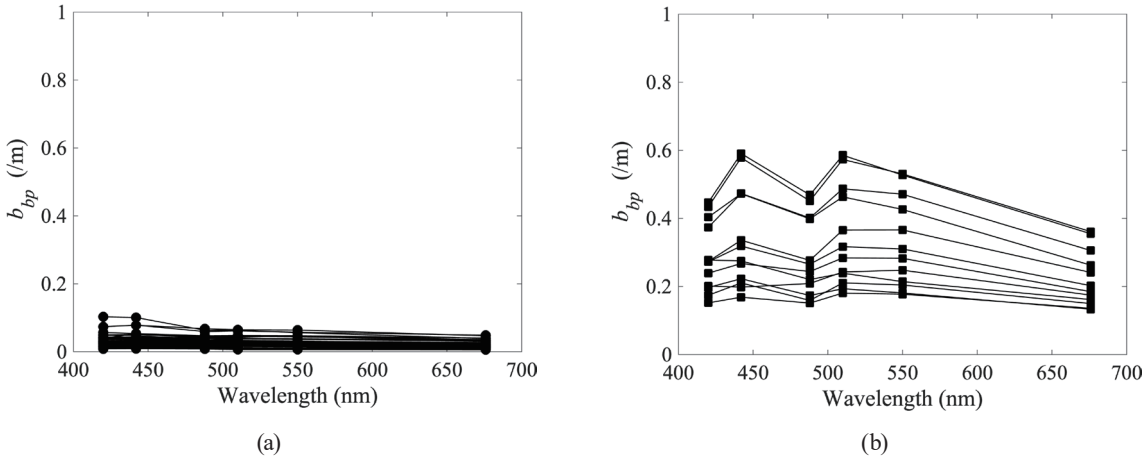

Fig. 3. Spectral distribution of b_{bp} in each water body. (a) Tokyo Bay, (b) Lake Kasumigaura, and (c) Upper Gulf of Thailand.

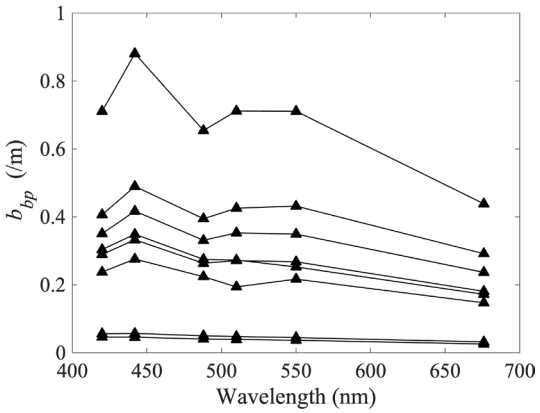

(c)

Fig. 3. (Continued) Spectral distribution of b_{bp} in each water body. (a) Tokyo Bay, (b) Lake Kasumigaura, and (c) Upper Gulf of Thailand.

comparison of Chl-a among the three water bodies, the average value in the Upper Gulf of Thailand is approximately half of the levels observed in Tokyo Bay and Lake Kasumigaura. The maximum values of ISS are 26.0 mg/l in Lake Kasumigaura and 28.1 mg/l in the Upper Gulf of Thailand, which are higher than the maximum value of 12.5 mg/l in Tokyo Bay. The percentages of ISS relative to TSS are 48% in Tokyo Bay, 73% in Lake Kasumigaura, and 83% in the Upper Gulf of Thailand. It is noteworthy that even in Lake Kasumigaura, the proportion of ISS is relatively high, similar to the Upper Gulf of Thailand. This can be attributed to rainfall observed on the days preceding the observation, specifically, on July 10 and August 7 to 9, 2018, which resulted in the influx of ISS from rivers and the resuspension of sediments owing to wind action. In the Upper Gulf of Thailand, the high concentration of ISS near the river mouth is considered to be the main cause of increased light scattering and the subsequent increase in R_{rs} intensity.

3.2 Calculation results of R_{rs} using radiative transfer simulation

Figure 4 shows the comparison between the calculated values and measured values of R_{rs} obtained through radiative transfer simulations using the measured values of b_{bp} after applying the σ correction method. Table 2 presents the error metrics (*Bias*, *RMSLE*) for each water body and wavelength based on the results in Fig. 4. Analyzing the *Bias* for each wavelength in each water body, we observed that Lake Kasumigaura and the Upper Gulf of Thailand had positive *Bias* values across the six wavelengths, indicating an overall overestimation compared with Tokyo Bay. Tokyo Bay, as indicated in Table 2, is a water body where the effect of light absorption is significant, resulting in lower R_{rs} values at each wavelength. The average *RMSLE* for each wavelength in Tokyo Bay was 0.197, the lowest among the three water bodies. On the other hand, Lake Kasumigaura and the Upper Gulf of Thailand had higher *RMSLE* values of 0.533 and 0.288, respectively. In Tokyo Bay, the calculated R_{rs} values were overestimated compared with the measured values at shorter wavelengths (420, 442, and 480 nm), while they were underestimated at longer wavelengths (510, 550, and 676 nm). In Lake Kasumigaura and

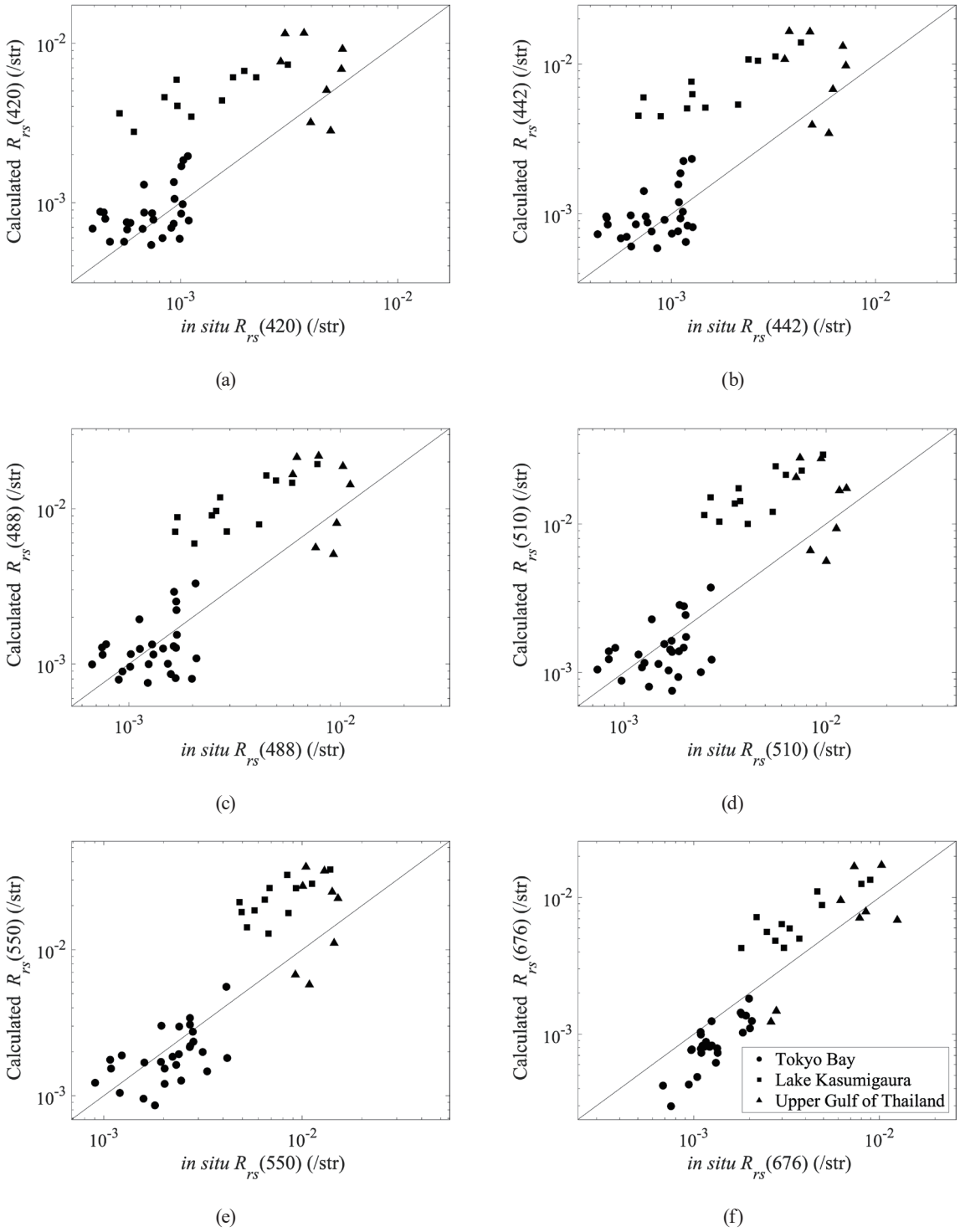

Fig. 4. Calculated and measured values of R_{rs} at six wavelengths obtained using the radiative transfer model. The results in the figure represent the following wavelengths: (a) 420, (b) 442, (c) 488, (d) 510, (e) 550, and (f) 676 nm. The circles represent Tokyo Bay, squares represent Lake Kasumigaura, and triangles represent the Upper Gulf of Thailand.

Table 2
Results of Bias and *RMSLE* for the calculated values of R_{rs} and the measured values obtained using the radiative transfer model. The results are presented for Tokyo Bay, Lake Kasumigaura, and the Upper Gulf of Thailand at six different wavelengths.

	Wavelength (nm)	Tokyo Bay	Lake Kasumigaura	Upper Gulf of Thailand
Bias ($\times 10^{-3}$)	420	0.156	3.536	2.942
	442	0.163	5.724	4.698
	480	0.018	7.494	5.479
	510	−0.097	12.049	6.743
	550	−0.250	15.140	9.038
	676	−0.408	3.401	1.278
RMSLE	420	0.170	0.629	0.332
	442	0.181	0.664	0.369
	480	0.184	0.524	0.327
	510	0.185	0.567	0.333
	550	0.179	0.488	0.329
	676	0.203	0.301	0.242

the Upper Gulf of Thailand, the *Bias* values were positive for all wavelengths, indicating an overall overestimation of R_{rs} compared with the measured values, and the relative errors were also found to be larger. These results confirm that the reproducibility of the radiative transfer calculations is lower in water bodies with a significant effect of light scattering.

3.3 Estimation results of b_{bp} using the inversion model

Using the inversion model, specifically, the QAA, we estimated b_{bp} at six different wavelengths based on the R_{rs} values for each water area. The estimated values and the measured values are shown in Fig. 5. Table 3 presents the *Bias* and *RMSLE* for each water area at the six wavelengths. In this case, the measured values of b_{bp} on the horizontal axis are the results of applying the previous σ correction. For Tokyo Bay, the average *RMSLE* at the six wavelengths is 0.20, indicating a relatively high accuracy in the estimation. On the other hand, for Lake Kasumigaura and the Upper Gulf of Thailand, the average *RMSLE* at the six wavelengths is 0.72 and 0.35, respectively, which is 1.5 to 3.5 times larger than that for Tokyo Bay. Moreover, in all cases, the *Bias* values are negative, indicating an underestimation of the estimated values compared with the measured values. These results suggest the possibility of errors in the estimation using inversion, particularly for Lake Kasumigaura and the Upper Gulf of Thailand, which have distinct characteristics with higher values of b_{bp}. However, as pointed out by de Carvalho *et al.*[12] and Doxaran *et al.*,[5] the uncertainty of the measurement results at the measurement stage, including corrections for the optical path length of b_{bp} measured values, may also affect the validation results.

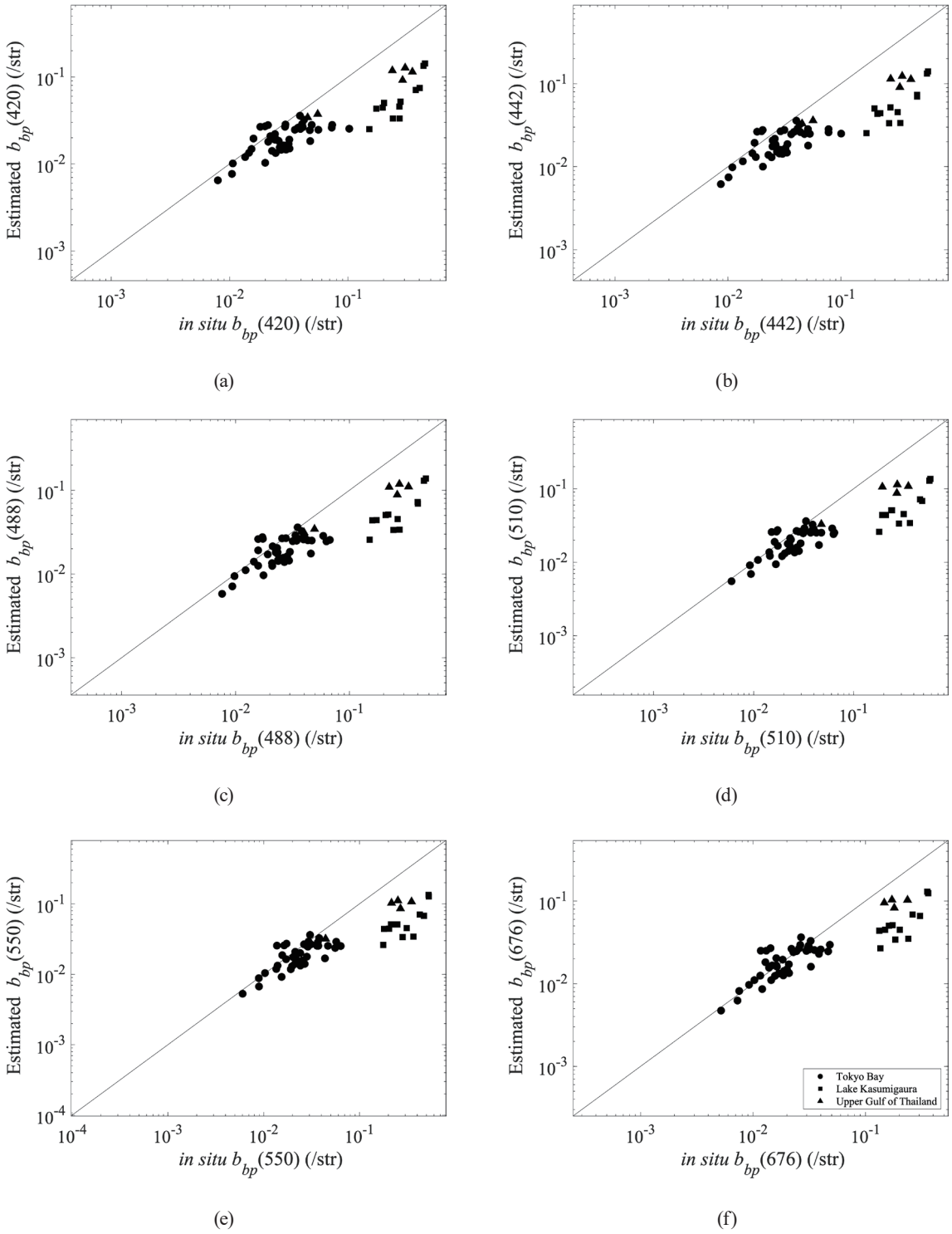

Fig. 5. Estimated and measured values of b_{bp} at six different wavelengths using the inversion model. Results at (a) 420, (b) 442, (c) 488, (d) 510, (e) 550, and (f) 676 nm. The circles represent Tokyo Bay, the squares represent Lake Kasumigaura, and the triangles represent the Upper Gulf of Thailand.

Table 3
Results of Bias and *RMSLE* for the estimated values of b_{bp} calculated using the inversion model shown in Fig. 5, compared with the measured values. The results are presented for Tokyo Bay, Lake Kasumigaura, and the Upper Gulf of Thailand at six different wavelengths.

	Wavelength (nm)	Tokyo Bay	Lake Kasumigaura	Upper Gulf of Thailand
Bias ($\times 10^{-2}$)	420	−1.167	−22.440	−12.613
	442	−1.316	−28.030	−16.071
	480	−0.816	−22.307	−11.482
	510	−0.792	−28.371	−11.612
	550	−0.690	−26.716	−11.628
	676	−0.198	−16.200	−5.858
RMSLE	420	0.229	0.708	0.356
	442	0.245	0.774	0.417
	480	0.197	0.701	0.346
	510	0.195	0.782	0.354
	550	0.186	0.765	0.358
	676	0.142	0.605	0.234

3.4 Calculation results of R_{rs} using b_{bp} with and without σ correction

To understand the effect of σ correction in Hydroscat-6P backscattering measurements on b_{bp}, the measured values of b_{bp} were used as input to Hydrolight to calculate R_{rs} at six different wavelengths, considering two cases: one with σ correction applied and the other without σ correction. The relationship between the calculated R_{rs} values and the measured values is shown in Fig. 6. Additionally, Table 4 presents the error metrics for the calculated R_{rs} values and measured values in these two cases and for each water body. Focusing on the results for Tokyo Bay at each wavelength in Fig. 6, we observed that the variations in *Bias* and *RMSLE* owing to the application or absence of σ correction are small. However, for Lake Kasumigaura and the Upper Gulf of Thailand, when σ correction is applied, *Bias* is positive and large, indicating an overestimation. Furthermore, except for 676 nm in the Upper Gulf of Thailand, in the absence of σ correction, *Bias* and *RMSLE* are significantly smaller than in cases with σ correction, and the distribution of R_{rs} approaches the 1:1 line. In the case of the Upper Gulf of Thailand, the calculated R_{rs} values exhibit positive *Bias* in all wavelengths when σ correction is applied, whereas in the absence of correction, all *Bias* values are negative. This indicates a transition from an overestimation tendency to an underestimation tendency due to the absence of σ correction. On the other hand, in the case of Lake Kasumigaura, the calculated R_{rs} values are already overestimated compared with the measured values at all six wavelengths in the absence of σ correction. The application of σ correction further amplifies the overestimation, resulting in an approximately 2.5-fold increase in *RMSLE*. This suggests that in highly turbid water bodies with significant light scattering, the excessive correction of light attenuation due to σ correction may lead to an overestimation of the b_{bp} measurement.

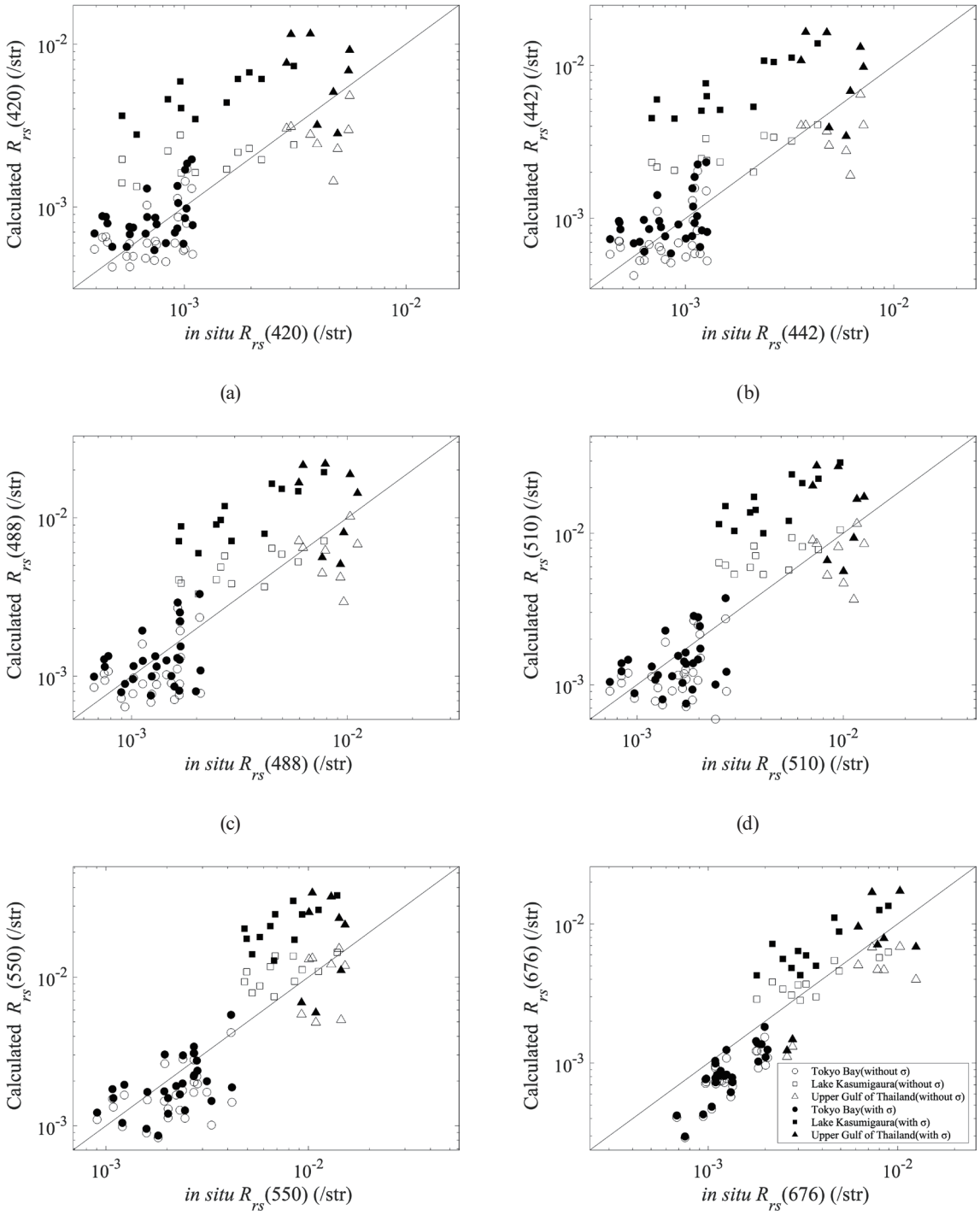

Fig. 6. R_{rs} values calculated using the radiative transfer model with the measured b_{bp} values are compared with the actual measurements. The results at six different wavelengths are shown: (a) 420, (b) 442, (c) 488, (d) 510, (e) 550, and (f) 676 nm. The circles represent Tokyo Bay, squares represent Lake Kasumigaura, and triangles represent the Upper Gulf of Thailand. The unfilled symbols represent the case with σ correction, whereas the filled symbols represent the case without σ correction.

Table 4
Bias and *RMSLE* for the relationship between calculated R_{rs} values and actual measurements at six wavelengths, using measured b_{bp} values as input for the radiative transfer model in two cases: with and without σ correction.

		Tokyo Bay		Lake Kasumigaura		Upper Gulf of Thailand	
	Wavelength (nm)	with σ corr.	without σ corr.	with σ corr.	without σ corr.	with σ corr.	without σ corr.
Bias ($\times 10^{-3}$)	420	0.156	−0.060	3.536	0.605	2.942	−1.432
	442	0.163	−0.088	5.724	0.924	4.698	−1.642
	480	0.018	−0.239	7.494	1.239	5.479	−2.450
	510	−0.097	−0.361	12.049	2.353	6.743	−2.317
	550	−0.250	−0.550	15.140	3.124	9.038	−1.942
	676	−0.408	−0.493	3.401	−0.020	1.278	−2.935
RMSLE	420	0.170	0.186	0.629	0.306	0.332	0.254
	442	0.181	0.201	0.664	0.299	0.369	0.247
	480	0.184	0.227	0.524	0.225	0.327	0.250
	510	0.185	0.231	0.567	0.239	0.333	0.233
	550	0.179	0.216	0.488	0.199	0.329	0.225
	676	0.203	0.233	0.301	0.127	0.242	0.284

4. Discussion

4.1 Correction of light attenuation due to optical path length in backscattering measurements

As shown in Fig. 6, it is suggested that the measured b_{bp} values may be overestimated due to the excessive correction of light attenuation caused by the σ correction. As indicated by Eq. (1), the σ coefficient is expressed exponentially and always has a value greater than or equal to 1. This correction method adds the light attenuation component in the optical path length cumulatively and is a reasonable formulation. However, in highly turbid waters, the β_u value, which is the volume scattering function before σ correction, may already be overestimated during the measurement stage, resulting in a further increase in b_{bp} through the σ correction. The exact factors contributing to the overestimation of β_u at this optical path length are unclear, but it is possible that the effects of multiple scattering, caused by the presence of densely packed particulate matter in highly turbid waters, lead to a shorter effective optical path length between the sensors, affecting β_u or the measured b_{bp} value before the σ correction. Zhang *et al.*[22] evaluated how fixed-angle backscattering sensors detect photons with specific scattering angles in situations where multiple scattering occurs, using Monte Carlo simulations. Under the conditions of a = 2 (/m) and Fournier–Forand phase function (B = 0.022), Hydroscat-6 (not 6P) showed that the proportion of detected scattered photons that were due to multiple scattering increased for b values greater than 5 (/m), reaching 92% at b = 20 (/m). It was also mentioned that multiple scattering can lead to an extension of the optical path length, causing changes in the scattering angles of detected light. On the other hand, an increase in absorption results in a shorter optical path length, and variations in the size of absorption and scattering lead to changes in the scattering angles of detected light. Considering the effect of multiple scattering on sensor detection based on the magnitude of absorption and scattering in the measurement area, it is

important to appropriately evaluate β_u. In this study, the average values of $b_{bp}(550)$ in the surveyed areas of Lake Kasumigaura and the Upper Gulf of Thailand were 0.34 and 0.29 (/m), respectively, which is more than 10 times higher than Tokyo Bay's 0.03 (/m). In water areas with such significant light scattering, it can be inferred that the effect of multiple scattering cannot be ignored. Furthermore, in the three study areas, the average values of TSS were 10.8, 25.5, and 14.6 (mg/l) for Tokyo Bay, Lake Kasumigaura, and the Upper Gulf of Thailand, respectively. The maximum values were 23.4, 33.8, and 32.6 (mg/l), respectively, indicating high concentrations. The proportions of ISS to TSS were 48% in Tokyo Bay, 72% in Lake Kasumigaura, and 78% in the Upper Gulf of Thailand. Notably, Lake Kasumigaura and the Upper Gulf of Thailand exhibited significantly higher proportions of ISS, which is considered to be the primary factor contributing to the heightened light scattering observed in these regions.

In addition, Doxaran *et al.*[5] addressed the uncertainties in b_{bp} measurements in highly turbid waters and proposed a new correction method for light attenuation. Additionally, their method, which utilizes the Fournier–Forand function, has demonstrated improved reproducibility of radiative transfer calculations in Monterey Bay, California, where harmful algal blooms occur.[6] However, they used Hydroscat-4, which has a shorter optical path length than Hydroscat-6P used in this research, and reported that the difference in optical path length has a significant impact on the degree of multiple scattering effects. Therefore, in future studies, a correction method is needed to reduce the overestimation of light scattering for sensors with longer optical path lengths, such as Hydroscat-6P, in highly turbid waters where multiple scattering occurs.

4.2 Uncertainties in radiative transfer calculations

While we examined the uncertainties associated with the measurement of the b_{bp} in this study, there are remaining challenges in understanding the uncertainties related to the measurement of the absorption coefficient, the setting of the backscattering probability in the radiative transfer model, the setting of the scattering phase function, and the vertical distribution of IOPs. The measured values of the absorption coefficient used as input in the radiative transfer model in this study were obtained using a spectrophotometer in transmittance mode. Boss *et al.*[23] recommends spectrophotometry in internally-mounted cuvettes inside an integrating sphere (IS-mode) to minimize uncertainties caused by scattering losses for the accurate measurement of the particle absorption coefficient. It is particularly important to pay attention to the quality of measured absorption coefficients in highly turbid waters. Additionally, in the filter pad method for absorption coefficient measurement, a pathlength amplification factor β, namely, β correction factor, is applied to correct for various scattering effects occurring between particles and filters or within filters. In this study, the β correction factor from Stramski *et al.*[24] was used, and the differentiation of the β correction factor usage across multiple water bodies has not been implemented, so evaluating its impact in the future is necessary. Moreover, regarding the vertical distribution of IOPs, since the target water bodies mainly consist of highly turbid water with low transparency, a uniform distribution of IOPs was assumed. However, the effects of changes in the vertical distribution on radiation have been reported,[25] and this should be

considered as a future research challenge. Furthermore, in this study, the calculation of b_{bp} was performed by fixing χ based on the average theorem of integrating from a single angle of the VSF. However, for highly turbid water where the angular distribution of the VSF can become complex, considering variations in χ is necessary. According to Xiong *et al.*,[26] approximately 71% of the uncertainty in R_{rs} attributed to the shape of the VSF can be explained by the backscattering probability of particles (B_p), approximately 90% by the scattering phase function, and approximately 97% by the conversion coefficient χ_p for particles. Additionally, the applicability of analytical functions such as the Fournier–Forand function in highly turbid water is known to be uncertain,[27,28] and further research on its applicability is needed in the future.

4.3 Overestimation in backscattering measurements and its proportion

As shown in Sect. 3.4, in highly turbid water bodies such as Lake Kasumigaura and the Upper Gulf of Thailand, the calculated R_{rs} values obtained from the radiative transfer model using IOPs as inputs were found to be overestimated compared with the measured values. This suggests the possibility of overestimation in scattering measurements, including the σ correction. To investigate the proportion of overestimation caused by excessive scattering, the b_{bp} values obtained from the σ corrected measurements were multiplied by a constant A ranging from 0.01 to 1 with an interval of 0.01. The calculated R_{rs} values using these modified inputs in Hydrolight were compared with the measured values to determine the proportion of overestimation using the *RMSLE* metric. Table 5 shows the results of the constants A corresponding to the minimum *RMSLE* for each wavelength in each water body. Examining the results, we found that for Tokyo Bay, the *RMSLE* between the calculated R_{rs} values and the measured values was minimized when using the σ-corrected b_{bp} values (A = 1) for wavelengths of 510, 550, and 676 nm. This suggests that in Tokyo Bay, where light absorption is dominant, the impact of scattering measurement uncertainty on the calculation results of R_{rs} is limited, and the conventional σ correction method appropriately compensates for the effect of light attenuation. In contrast, in Lake Kasumigaura and the Upper Gulf of Thailand, characterized by significant light scattering, there was a potential overestimation of light scattering in 64–75% and 29–39% proportions, respectively, for the five wavelengths excluding 676 nm. The cause of this overestimation could be attributed to multiple scattering effects occurring in the optical path length between sensors. The proportions of overestimation were specific to each water body, indicating their unique characteristics within the limited sample range of this study. Additionally, for Lake Kasumigaura and the Upper Gulf of Thailand, the proportion of overestimation at 676 nm, in the near-infrared region, was smaller than at other wavelengths, suggesting a relationship with the suitability of

Table 5
The optimal value of constant A, which minimized the *RMSLE* between the calculated and measured R_{rs} values, was determined for each water body and wavelength combination using the σ-corrected b_{bp} measurements.

Wavelength (nm)	420	442	480	510	550	676
Tokyo Bay	0.81	0.81	0.97	1.00	1.00	1.00
Lake Kasumigaura	0.27	0.25	0.35	0.31	0.36	0.59
Upper Gulf of Thailand	0.65	0.61	0.70	0.69	0.71	1.00

chlorophyll fluorescence models. Furthermore, as mentioned in Sect. 4.2, the results of the proportion of A are also influenced by the computational conditions of the radiative transfer calculations.

Next, the QAA inversion algorithm was used to estimate b_{bp} using the measured R_{rs} values. Figure 7 shows the relationship between the measured b_{bp} values, including the proportion of overestimation, and the estimated b_{bp} values. The error metrics are presented in Table 6. From the results for Lake Kasumigaura and the Upper Gulf of Thailand, the relationship between the measured and calculated b_{bp} values using the conventional method showed negative biases of −0.24 and −0.115, indicating underestimation. However, when considering the proportion of overestimation in the measured b_{bp} values, the biases were still negative (−0.042 and −0.058), but with lower *RMSLE* than the conventional method. This suggests that the distribution of b_{bp} values approached the 1:1 line. These findings indicate that overestimation in b_{bp} measurements can significantly affect the accuracy validation of the inversion algorithm. These findings emphasize the importance of improving the accuracy of b_{bp} measurements in the performance evaluation of inversion algorithms targeting highly turbid water bodies and the need to carefully assess the quality of previously acquired measured data.

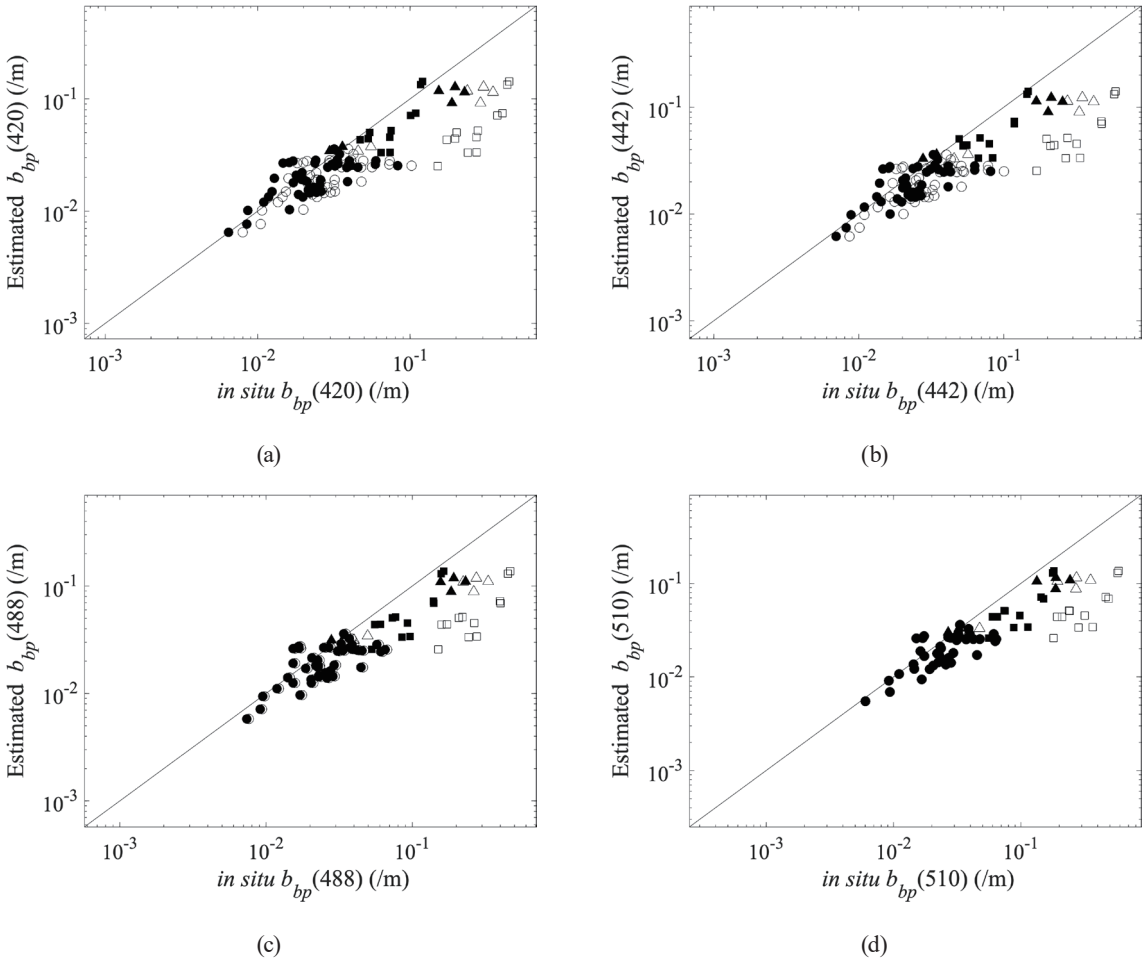

Fig. 7. Estimated values of b_{bp} obtained from the inversion model and the measured values of b_{bp} multiplied by a constant A. The wavelengths (a) 420, (b) 442, (c) 488, (d) 510, (e) 550, and (f) 676 nm indicate the measurement wavelengths of b_{bp}.

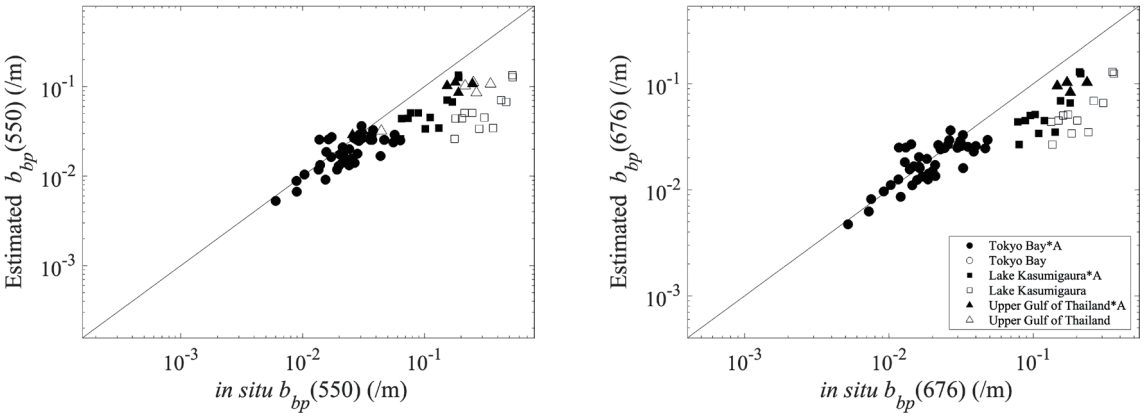

(e) (f)

Fig. 7. (Continued) Estimated values of b_{bp} obtained from the inversion model and the measured values of b_{bp} multiplied by a constant A. The wavelengths (a) 420, (b) 442, (c) 488, (d) 510, (e) 550, and (f) 676 nm indicate the measurement wavelengths of b_{bp}.

Table 6
Results of *Bias* and *RMSLE* for the estimated b_{bp} values obtained from the inversion model, measured values, and measured values multiplied by constant A. Results are presented for Tokyo Bay, Lake Kasumigaura, and the Upper Gulf of Thailand at six wavelengths.

		Tokyo Bay		Lake Kasumigaura		Upper Gulf of Thailand	
	Wavelength (nm)	*in situ* b_{bp}	*in situ* $b_{bp} \times A$	*in situ* b_{bp}	*in situ* $b_{bp} \times A$	*in situ* b_{bp}	*in situ* $b_{bp} \times A$
Bias ($\times 10^{-2}$)	420	−1.167	−0.552	−22.440	−1.504	−12.613	−5.141
	442	−1.316	−0.677	−28.030	−2.356	−16.071	−6.485
	480	−0.816	−0.731	−22.307	−3.810	−11.482	−5.575
	510	−0.792	−0.792	−28.371	−4.578	−11.612	−5.537
	550	−0.690	−0.690	−26.716	−5.727	−11.628	−5.995
	676	−0.198	−0.198	−16.200	−7.099	−5.858	−5.858
RMSLE	420	0.229	0.176	0.708	0.178	0.356	0.199
	442	0.245	0.185	0.774	0.201	0.417	0.237
	480	0.197	0.189	0.701	0.265	0.346	0.214
	510	0.195	0.195	0.782	0.291	0.354	0.220
	550	0.186	0.186	0.765	0.338	0.358	0.234
	676	0.142	0.142	0.605	0.383	0.234	0.234

5. Conclusions

In this study, optical and water quality observations were conducted in multiple high-turbidity coastal areas with different optical characteristics. Tokyo Bay exhibited eutrophication with a dominance of phytoplankton and a significant effect of light absorption rather than scattering. On the other hand, Lake Kasumigaura had a mixture of organic and inorganic substances, whereas the Upper Gulf of Thailand was characterized by the prevalence of inorganic suspended matter, both exhibiting significant light scattering. By using the measured

values of b_{bp} and absorption coefficients obtained from each area as input values, R_{rs} was calculated using a radiative transfer model and compared with the measured values to assess the uncertainty of b_{bp} measurements. The results showed that the reproducibility of R_{rs} had different trends for each water area, particularly in the highly scattering waters of Lake Kasumigaura and the Upper Gulf of Thailand, where the calculated values were found to be overestimated compared with the measured values. This overestimation was observed even at the stage of calculating R_{rs} with the input of precorrection β_u values and further magnified by the application of σ correction.

Furthermore, the impact of σ correction on b_{bp} measurements was assessed by comparing the calculated R_{rs} values with and without σ correction using the respective b_{bp} measurements as input in Hydrolight. The results indicated that in the highly scattering waters of Lake Kasumigaura and the Upper Gulf of Thailand, the calculated R_{rs} values without σ correction were consistently higher than the measured R_{rs} values at all wavelengths. This suggests a potential overestimation of the detected scattering light owing to multiple scattering in the optical path between Hydroscat-6P sensors when suspended particles are present at high density. Moreover, the percentage of overestimation was found to be 64–75% for Lake Kasumigaura and 29–39% for the Upper Gulf of Thailand, highlighting its significant impact on the accuracy assessment of b_{bp} estimation using inversion models. These findings underline the uncertainty of b_{bp} measurements in high-turbidity waters and emphasize the need for developing correction methods that appropriately account for the optical path length of light attenuation processes. Additionally, they suggest the importance of carefully evaluating the quality of past measured data when assessing the performance of inversion algorithms.

Acknowledgments

This work was supported by JSPS KAKENHI Grant Numbers JP20K14836 and JP22H05716. In addition, this work was also supported by the Japan Aerospace Exploration Agency (JAXA) Global Change Observation Mission-Climate (GCOM-C) to PI No. ER3GCF301.

References

1 P. J. Werdell, L. I. W. McKinna, E. Boss, S. G. Ackleson, S. E. Craig, W. W. Gregg, Z. Lee, S. Maritorena, C. S. Roesler, C. S. Rousseaux, D. Stramski, J. M. Sullivan, M. S. Twardowski, M. Tzortziou, and X. Zhang: Prog. Oceanogr. **160** (2018) 186. https://doi.org/10.1016/j.pocean.2018.01.001
2 G. Neukermans, H. Loisel, X. Mériaux, R. Astoreca, and D. McKee: Limnol. Oceanogr. **57** (2012) 124. https://doi.org/10.4319/lo.2012.57.1.0124
3 M. Defoin-Platel and M. Chami: J. Geophys. Res. Oceans. **112** (2007). https://doi.org/10.1029/2006JC003847
4 A. Najah and M. R. Al-Shehhi: Remote Sens. Earth Syst. Sci. **4** (2021) 235. https://doi.org/10.1007/s41976-022-00068-3
5 D. Doxaran, E. Leymarie, B. Nechad, A. Dogliotti, K. Ruddick, P. Gernez, and E. Knaeps: Opt. Express. **24** (2016) 3615. https://doi.org/10.1364/OE.24.003615
6 N. Tuchow, B. J. Broughton, and R. Kudela: Opt. Express. **24** (2016) 18559. https://doi.org/10.1364/OE.24.018559
7 G. Chang, A. Barnard, and J. R. V. Zaneveld: Appl. Opt. **46** (2007) 7679. https://doi.org/10.1364/AO.46.007679
8 J. Huang, L. Chen, X. Chen, and Q. Song: J. Oceanogr. **69** (2013) 713. https://doi.org/10.1007/s10872-013-0202-8
9 H. Loisel, D. Stramski, D. Dessaill, C. Jamet, L. Li, and R. A. Reynolds: J. Geophys. Res.: Oceans **123** (2018) 2141. https://doi.org/10.1002/2017JC013632

10 T. Oishi: Appl. Opt. **29** (1990) 4658. https://doi.org/10.1364/AO.29.004658
11 R. A. Maffione and D. R. Dana: Appl. Opt. **36** (1997) 6057. https://doi.org/10.1364/AO.36.006057
12 L. A. S. de Carvalho, C. C. F. Barbosa, E. M. L. de Moraes Novo, and C. de Moraes Rudorff: Remote Sens. Environ. **157** (2015) 123. https://doi.org/10.1016/j.rse.2014.06.018
13 B. Bulgarelli, G. Zibordi, and J. F. Berthon: Appl. Opt. **42** (2003) 5365. https://doi.org/10.1364/AO.42.005365
14 C. L. Gallegos, R. J. Davies-Colley, and M. Gall: Limnol. Oceanogr. **53** (2008) 2021. https://doi.org/10.4319/lo.2008.53.5.2021
15 H. Kobayashi, M. Toratani, S. Matsumura, A. Siripong, T. Lirdwitayaprasit, and P. Jintasaeranee: Int. Arch. Photogramm. Remote Sens. Spat. Inf. Sci, (2010) 997.
16 HOBI-labs Inc.: Hydroscat-6p Spectral Backscattering Sensor and Fluorometer User's Manual (HOBI-labs_ Inc, Washington, 2010) Revision J, 9.6.
17 A. L. Whitmire, W. S.Pegau, L. Karp-Boss, E. Boss, and T. J. Cowles: Opt. Express. **18** (2010) 15073. https://doi.org/10.1364/OE.18.015073
18 J. D. Hedley and C. D. Mobley: HYDROLIGHT 6.0 ECOLIGHT 6.0 Technical Documentation. (Numerical Optics Ltd. Tiverton, UK, 2021) version 6.0.0.
19 G. R. Fournier and M. Jonasz: SPIE **3761** (1999) 62. https://doi.org/10.1117/12.366488
20 A. Gilerson, J. Zhou, S. Hlaing, I, Ioannou, B. Gross, F. Moshary, and S. Ahmed: Opt. Express. **16** (2008) 2446. https://doi.org/10.1364/OE.16.002446
21 Update of the Quasi-Analytical Algorithm (QAA_v6): https://www.ioccg.org/groups/Software_OCA/QAA_v6_2014209.pdf (accessed November 2022).
22 X. Zhang, E. Leymarie, E. Boss, and L. Hu: Appl. Opt. **60** (2021) 8676. https://doi.org/10.1364/AO.437735
23 E. Boss, N. Haëntjens, S. G. Ackleson, B. Balch, A. Chase, G. Dall'Olmo, S. Freeman, Y. Liu, J. Loftin, W. Neary, N. Nelson, M. Novak, W. Slade, C. Proctor, P. Tortell, and T. Westberry: IOCCG Ocean Optics and Biogeochemistry Protocols for Satellite Ocean Colour Sensor Validation (2019).
24 D. Stramski, R. Reynolds, S. Kaczmarek, J. Uitz, and G. Zheng: Appl. Opt. **54** (2015) 6763. https://doi.org/10.1364/AO.54.006763
25 B. Sundarabalan, P. Shanmugam, and S. Manjusha: J. Quant. Spectrosc. Radiat. Transfer. **121** (2013) 30. https://doi.org/10.1016/j.jqsrt.2013.01.016
26 Y. Xiong, X. Zhang, S. He, and D. J. Gray: Appl. Opt. **56** (2017) 6881. https://doi.org/10.1364/AO.56.006881
27 M. Chami, D. McKee, E. Leymarie, and G. Khomenko: Appl. Opt. **45** (2006) 9210. https://doi.org/10.1364/AO.45.009210
28 M. Talaulikar, T. Suresh, E. Desa, and A. Inamdar: J. Indian Soc. Remote Sens. **43** (2015) 163. https://doi.org/10.1007/s12524-014-0393-5

About the Authors

Hiroto Higa received his B.S. degree from Tokyo University of Science, Japan, in 2010 and his M.S. and Ph.D. degrees from The University of Tokyo, Japan, in 2012 and 2015, respectively. From 2016 to 2022, he was an assistant professor at Yokohama National University, Japan. Since 2023, he has been an associate professor at Yokohama National University. His research interests are in water environmental engineering and ocean color remote sensing. (higa@ynu.ac.jp)

Ryota Ideno received his B.S. degree from Yokohama National University, Japan, in 2022. Since 2022, he has been pursuing his master's degree at Yokohama National University. His research interests are in the measurement of backscattering coefficients of marine particles and radiative transfer simulation for the purpose of ocean color remote sensing. (ideno-ryota-dr@ynu.jp)

Salem Ibrahim Salem received his B.Sc. and M.Sc. degrees from Alexandria University, Egypt, in 2005 and 2010, respectively. He obtained his Ph.D. degree from The University of Tokyo, Japan in 2017. Following that, he served as a postdoctoral researcher at The University of Tokyo from 2017 to 2019. Since 2019, he has been a junior associate professor at Kyoto University of Advanced Science, Japan. His research interests lie in the field of environmental monitoring, remote sensing, and data science.
(salem.ibrahim@kuas.ac.jp; eng.salemsalem@gmail.com)

Hiroshi Kobayashi received his B.S., M.S., and Ph.D. degrees from Hokkaido University, Japan, in 1994, 1996, and 1999, respectively. From 1999 to 2010, he was an assistant professor at the University of Yamanashi, Japan. Since 2010, he has been an associate professor at the University of Yamanashi. His research interests are in ocean color remote sensing and measurement of atmospheric aerosol optical properties. (kobachu@yamanashi.ac.jp)